

Improved interferometric tracking of trapped particles using two frequency-detuned beams

Lars Friedrich and Alexander Rohrbach*

Laboratory for Bio- and Nano-Photonics, Institute for Microsystem Technology (IMTEK) University of Freiburg, Germany
*Corresponding author: rohrbach@imtek.uni-freiburg.de

Received February 25, 2010; accepted April 26, 2010;
posted May 14, 2010 (Doc. ID 124740); published May 28, 2010

For most optical tweezer applications, precise and reliable tracking of the trapped particle is an important requirement. Backfocal-plane interferometry is the fastest and most accurate tracking technique if the particle displacements are limited to half of the focal width. Especially for positive axial displacements, the nonlinear detector response can lead to incorrect tracking results. Here we show how the linear detection range around the trap center can be extended by a factor of 2 to 4 in the axial direction using a second frequency-detuned tracking focus that is generated by the same laser as the optical trap. Additionally, we show how the noise in the axial signal can be decreased significantly using a second detector. © 2010 Optical Society of America

OCIS codes: 120.0120, 140.7010, 260.3160, 290.0290.

In many microscopic studies, single-particle tracking (SPT) gives new insights into the structure and dynamics of biological samples that cannot be achieved with conventional imaging. Different tracking methods, varying in bandwidth and precision, are used depending on the specific assay. For small investigation volumes, backfocal-plane (BFP) interferometry [1] is the fastest and most precise SPT technique. It is commonly used in optical tweezer setups, where it exploits the interference pattern generated by the trapping light and the light scattered by the trapped particle. The technique can be applied to various problems in biological and soft matter research [2], as in tracking of molecular motor steps [3], following the transcription of DNA [4], or for imaging structured surfaces [5]. Since the trap is usually 6 to 10 times weaker in axial direction than in the lateral directions [6], axial displacements are usually larger than lateral displacements, and axial position detection is indispensable to obtaining correct tracking results.

For a particle located at the position $\mathbf{b} = (b_x, b_y, b_z)$ with respect to the trapping focus, the axial position signal $S_z(b_z)$ is generated by measuring the intensity in the BFP of a detection objective that collects the incident trapping light field \tilde{E}_i and the scattered light field \tilde{E}_s with a finite-detection NA. S_0 denotes the signal for the empty trap and S_{os} is the constant signal offset at the focal position:

$$S_z(\mathbf{b}, \text{NA}) = \frac{1}{S_0} \iint_{\text{NA}} |\tilde{E}_i + \tilde{E}_s(\mathbf{b})|^2 dA \approx S_{os} + g_z(\text{NA}) \cdot b_z. \quad (1)$$

The axial position signal $S_z(b_z)$ is a nonmonotonic sinusoidal function of the axial displacement of the trapped particle (Fig. 1). To find the axial displacement from the measured signals, it must be ensured that the particle moves inside the unique detection range, which is the region between the signal minimum and maximum. The displacements must be even smaller, if the usual linear detector response is to be used, i.e., $g_z = (\partial/\partial b_z)S_z(b_z)|_{b_z=b_{z0}} = \text{const}$. Because of radiation pressure, the trap center b_{z0} is slightly behind the laser focus so that external axial forces may push the trapped particle

easily into the nonlinear region of $S_z(b_z)$. This leads to underestimated particle displacements and wrong force measurements. Several methods have been developed to increase the linear detection range, including spatial filtering [7–9] and the application of separate trapping and tracking lasers. Here we present a method to increase the linear detection range by using two frequency detuned, orthogonally polarized foci of only one laser as separate trapping and tracking foci. Additionally, we show that the signal of a high-NA detector can be used as a reference. This way, the shape of the axial detection signal is improved and laser power instabilities are corrected for so that the signal-to-noise ratio is increased.

The experimental setup is similar to that in [6] and is shown in Fig. 1. The light of a 2 W 1064 nm laser (Smart Labor Systems, Berlin) passes an optical isolator FI (OFR-IO-3-1064-VHP, Laser 2000) and acousto-optic deflectors (DTSXY-400, AA Opto-Electronic), of which only the first one is used as an acousto-optic modulator (AOM). To increase pointing stability, the zeroth-order diffracted beam is coupled into a polarization-maintaining single-mode fiber, F (Schaeffter+Kirchhoff). It is used as the tracking beam (blue in Fig. 1); its power

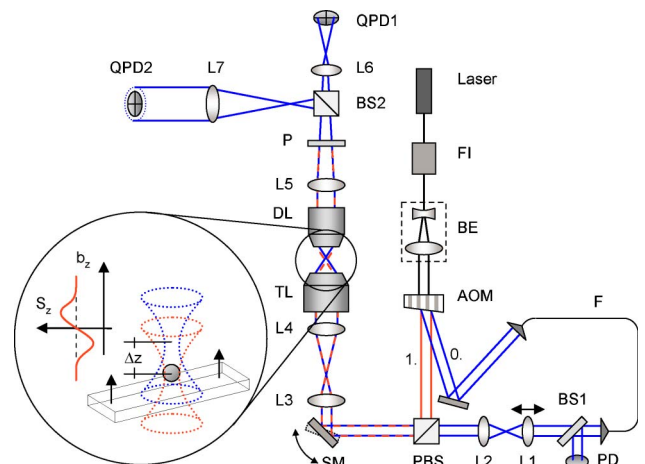


Fig. 1. (Color online) Experimental setup. Zeroth (blue / dark gray) and first (red / light gray) order diffracted beams of the AOM are combined by a polarizing beam splitter (PBS). Trapping lens (TL), scanning mirror (SM).

is stabilized by a feedback loop using an InGaAs photodiode (PD) (G8370-81, Hamamatsu) to sample the laser beam and an electronic noise eater (miniNE, TEM Messtechnik) to control the AOM. By moving lens L1, the axial position of the tracking focus can be adjusted. The first-order diffracted beam is used to generate the trapping focus and is orthogonally polarized with respect to the tracking beam. For the measurements, the powers of the trapping (tp) and the tracking (tk) focus are adjusted to $p_{tp} = 10 \cdot p_{tk}$. The interference pattern in the BFP of the detection lens (DL) is projected onto two detectors with different magnifications, leading to detection numerical apertures $NA_1 = 0.9$ and $NA_2 = 0.45$, and the polarizer (P) stops the trapping beam. Quadrant photodiodes (QPD) were used to allow lateral tracking, but, in this study, only the sum signals were evaluated.

To determine the trap center of a particle with respect to the detector response, a measurement as described in [10] is performed. A bead is trapped in 0.1 M NaCl solution. Then the coverslip is moved upward with a step size of 50 nm and a step time of 0.5 s while recording the detector signals. When the bead touches the coverslip, it attaches to the surface due to van der Waals forces. After moving the fixed bead through the peak of the axial detector response, the coverslip is moved downward again to sample the complete response (Fig. 2).

When the same beam is used for trapping and tracking (single-beam detection), there is a significant curvature of $S_z(b_z)$ at the trap center, as can be seen from the upper curves in Fig. 2. Typically, a linear fit to the detector signal [Eq. (1)] is used to determine the axial displacement of the trapped particle, leading to tracking errors

$\Delta b_z = (S_{os} + g_z \cdot b_z - S_z(b_z))/g_z$. A linear detection range can be defined by limiting the relative error $|\Delta b_z/(b_z - b_{z0})|$ to 10%. Since g_z is determined at b_{z0} , the position of the detector response with respect to the trap center has a strong influence on the linear range. For a 535 nm bead, this range is only 200 nm in size.

Therefore, a separate tracking beam is introduced and the telescope comprising L1 and L2 is used to adjust the relative axial position Δz of the tracking beam with respect to the trapping beam, as can be seen in Fig. 1. For the three considered bead sizes, we shifted L1 by $M^2 \Delta z = 0.7, 0.4,$ and 0.2 mm, corresponding to axial displacements of the detection signal of 400, 300, and 150 nm, with magnification M defined by the focal lengths of TL, L4, L3, and L2. For the 535 and 200 nm beads, the linear detection range was extended by a factor of 4 and 1.6 (Fig. 2). For the 1000 nm bead, the linear range was extended by only 100 nm, but as the limits of this range are strongly asymmetric about the trap center, this arrangement should be used when large positive bead displacements are expected.

The AOM is driven by an acoustic wave with frequency ω_{phonon} and generates an undiffracted beam and a first-order diffracted beam, which have slightly different frequencies, $\omega_{tp} = \omega_{tk} + \omega_{\text{phonon}}$. In the ideal case, the two foci are thus generated by two incident fields with different polarization and wavelengths $\mathbf{E}^{\parallel}(\omega_{tp}) + \mathbf{E}^{\perp}(\omega_{tk})$. While propagating through the measurement system, a fraction $d \approx 1/40$ of the power is depolarized so that the field $\tilde{\mathbf{E}}_D = \tilde{\mathbf{E}}^{\parallel}(\omega_{tp}) + \tilde{\mathbf{E}}^{\perp}(\omega_{tp}) + \tilde{\mathbf{E}}^{\parallel}(\omega_{tk}) + \tilde{\mathbf{E}}^{\perp}(\omega_{tk})$ with $\tilde{\mathbf{E}} = \tilde{\mathbf{E}}_i + \tilde{\mathbf{E}}_s$ at the exit of the detection lens, is composed of all combinations of polarization states and wavelengths. As the polarizer stops all parallel polarized light, the resulting signal,

$$S_z(b_z) = \frac{1}{S_0} \iint_{NA} (|\tilde{E}_i^{\perp}(\omega_{tp}) + \tilde{E}_s^{\perp}(\omega_{tp})|^2 + |\tilde{E}_i^{\perp}(\omega_{tk}) + \tilde{E}_s^{\perp}(\omega_{tk})|^2) dA, \quad (2)$$

is the superposition $S_z(b_z) = S_{z,tp}(b_z) + S_{z,tk}(b_z)$ of two signals generated by the tracking beam and the depolarized fraction $\tilde{\mathbf{E}}^{\perp}(\omega_{tp})$ of the trapping beam. The interference terms of tracking and trapping light are modulated with a beat frequency ω_{phonon} that lies beyond the bandwidth of the detector so that the detuned fields, in effect, add incoherently. While the trapping beam generates a standard detection signal $S_{z,tp}(b_z)$, the tracking beam generates the desired axially shifted signal $S_{z,tk}(b_z) = B \cdot S_{z,tp}(b_z - \Delta z)$ with a relative signal amplitude $B = (1 - d) \cdot p_{tk}/(d \cdot p_{tp}) \approx 4$. In the focal region, both signals are sinusoidal (see below) so that the shape of the resulting position signal is not affected by the unwanted trapping beam signal, except that it is shifted slightly less than Δz .

In the detection scheme described above, the signal-to-noise ratio of the axial position detection crucially depends on the laser power stability. While there are many different sources for intensity noise, the unwanted depolarized trapping light with power $d \cdot p_{tp}$ adds additional noise because it is not stabilized. In the following, we describe a method to correct for intensity instabilities

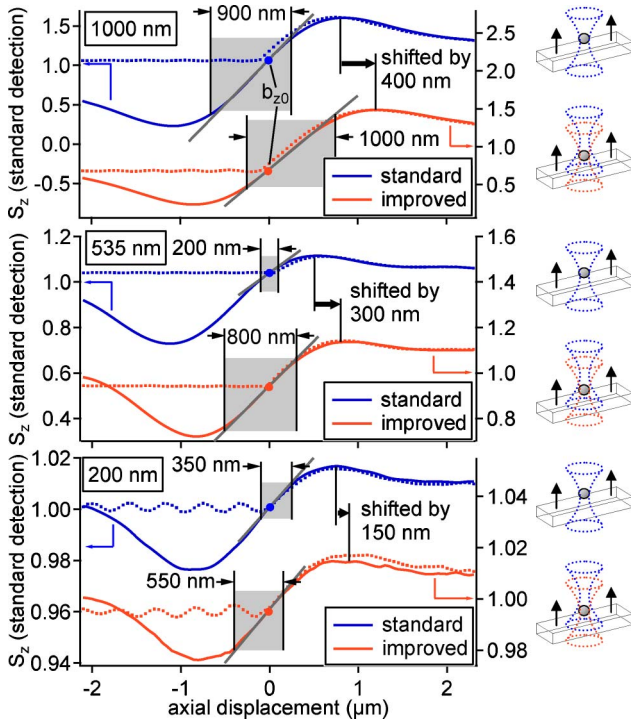


Fig. 2. (Color online) Low-NA single beam signals (blue / dark gray) and signals with separate tracking beam (red / light gray) for PS beads with different diameters. Dotted traces show signals $S_z(b_{z0})$ generated while fixing the bead to the coverslip, revealing the trap center b_{z0} . Straight lines indicate linear fits, and gray rectangles show the linear detection range.

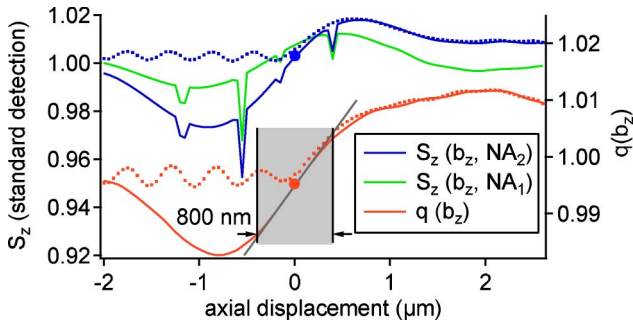


Fig. 3. (Color online) Axial signals for a PS bead, diameter 200 nm. The upper graphs show the signals for different detection NAs ($NA_1 = 0.9$ and $NA_2 = 0.45$), both for single beam detection. Intensity reductions cancel in the ratio $q(b_z)$ (red, lower graphs) of the two signals. A larger linear and unique detection region is obtained.

in the axial detection signal in general that can also be applied here. Figure 3 shows the axial detector response for a 200 nm diameter polystyrene (PS) bead that has a peak-to-peak modulation of only 4%. During the measurement, the intensity feedback was disturbed four times on purpose, leading to intensity reductions of up to 2%, to show the effectiveness of the method.

The intensity distribution $I_D = |\vec{E}_D^\perp|^2$ on the detector can be expressed in terms of the incident light I_i and the light scattered by the trapped particle I_s , which has a relative phase of $\Delta\varphi$ with respect to the incident field:

$$I_D = I_i + I_s + 2\sqrt{I_i I_s} \cos(\Delta\varphi). \quad (3)$$

The intensity of the scattered light can be expressed as a fraction of the incident intensity $I_s = \eta I_i$, with an efficiency parameter $0 < \eta(b_z) < 1$. For a particle located on the optical axis, the phase difference can be split into a constant part, $\Delta\varphi_b$, that depends on the shape of the scattering particle and a part that is approximately proportional to the particle's axial displacement, $\Delta\varphi_D \approx \beta b_z$, which arises from the Gouy phase shift of the focused incident light field [1]. With the fluctuating incident intensity $I_i(t)$, the detector intensity can be rewritten as

$$I_D(b_z) \approx I_i(t)(1 + \eta + 2\sqrt{\eta} \cos(\Delta\varphi_b + \beta b_z)). \quad (4)$$

For Rayleigh particles, $\Delta\varphi_b$ approaches $-\pi/2$ so that $\cos(\Delta\varphi_b + \beta b_z)$ becomes $\sin(\beta b_z)$, enabling axial tracking.

The laser intensity $I_i(t)$ is a common factor of all signals, regardless of the NA used, as can be seen from Eq. (4). Taking the ratio $q(b_z) = S_z(b_z, NA_2)/S_z(b_z, NA_1)$ of two signals generated with different NAs cancels $I_i(t)$.

β is reduced for high detection angles and eventually changes sign so that the correlation of intensity on the detector and axial displacement of the trapped particle becomes negative [8]. Thus, the signal recorded with the higher NA has a reduced sensitivity $g_z(NA_1) < g_z(NA_2)$ [7], so that $q(b_z)$ can be used for tracking (Fig. 3). The strong intensity modulations that were introduced on purpose are no longer present in the quotient.

In addition to the improvement in signal-to-noise ratio, $q(b_z)$ also has a strongly increased unique detection range. The high-NA signal has its positive peak at a lower axial displacement than the low-NA signal. In the peak region of $S_z(b_z, NA_2)$, the decreasing values of $S_z(b_z, NA_1)$ in the denominator shift the positive peak of $q(b_z)$ to higher values for b_z . The linear range is also extended from 350 (Fig. 2) to 800 nm (Fig. 3).

In conclusion, we demonstrated two ways of improving the axial position detection in BFP interferometry. The use of both diffraction orders of the acousto-optic modulator to generate separate tracking and trapping beams can be cheaper than the use of a second laser if acousto-optic intensity control is desirable for other applications, as well. The quotient of two signals from two diodes with different detection NAs increases the linear detection range significantly and, in addition, cancels out intensity noise. Remarkably, the two methods can be combined. We think that the methods presented in this letter enable new force and potential-probing experiments due to a significantly improved linear three-dimensional tracking range.

References

1. A. Pralle, M. Prummer, E. L. Florin, E. H. K. Stelzer, and J. K. H. Horber, *Microsc. Res. Tech.* **44**, 378 (1999).
2. P. Y. Wu, R. X. Huang, C. Tischer, A. Jonas, and E. L. Florin, *Phys. Rev. Lett.* **103**, 108101 (2009).
3. H. Kress, E. H. K. Stelzer, D. Holzer, F. Buss, G. Griffiths, and A. Rohrbach, *Proc. Natl. Acad. Sci. USA* **104**, 11633 (2007).
4. K. C. Neuman and S. M. Block, *Rev. Sci. Instrum.* **75**, 2787 (2004).
5. P. C. Seitz, E. H. K. Stelzer, and A. Rohrbach, *Appl. Opt.* **45**, 7309 (2006).
6. A. Rohrbach, C. Tischer, D. Neumayer, E. L. Florin, and E. H. K. Stelzer, *Rev. Sci. Instrum.* **75**, 2197 (2004).
7. A. Rohrbach, H. Kress, and E. H. K. Stelzer, *Opt. Lett.* **28**, 411 (2003).
8. J. K. Dreyer, K. Berg-Sorensen, and L. Oddershede, *Appl. Opt.* **43**, 1991 (2004).
9. H. Kress, E. H. K. Stelzer, G. Griffiths, and A. Rohrbach, *Phys. Rev. E* **71**, 061927 (2005).
10. M. J. Lang, C. L. Asbury, J. W. Shaevitz, and S. M. Block, *Biophys. J.* **83**, 491 (2002).